JOURNAL OF GEOPHYSICAL RESEARCH, VOL. 113, G04004, doi:10.1029/2007JG000650, 2008

Quantitative phenological observations of a mixed beech forest in northern Switzerland with digital photography

Hella Ellen Ahrends,[1] Robert Brügger,[1] Reto Stöckli,[2,3] Jürg Schenk,[1] Pavel Michna,[1] Francois Jeanneret,[1] Heinz Wanner,[1] and Werner Eugster[4]

Received 12 November 2007; revised 2 April 2008; accepted 23 July 2008; published 9 October 2008.

[1] Vegetation phenology has a strong influence on the timing and phase of global terrestrial carbon and water exchanges and is an important indicator of climate change and variability. In this study we tested the application of inexpensive digital visible-light cameras in monitoring phenology. A standard digital camera was mounted on a 45 m tall flux tower at the Lägeren FLUXNET/CarboEuropeIP site (Switzerland), providing hourly images of a mixed beech forest. Image analysis was conducted separately on a set of regions of interest representing two different tree species during spring in 2005 and 2006. We estimated the date of leaf emergence based on the levels of the extracted red, green and blue colors. Comparisons with validation data were in accordance with the phenology of the observed trees. The mean error of observed leaf unfolding dates compared with validation data was 3 days in 2005 and 3.6 days in 2006. An uncertainty analysis was performed and demonstrated moderate impacts on color values of changing illumination conditions due to clouds and illumination angles. We conclude that digital visible-light cameras could provide inexpensive, spatially representative and objective information with the required temporal resolution for phenological studies.

Citation: Ahrends, H. E., R. Brügger, R. Stöckli, J. Schenk, P. Michna, F. Jeanneret, H. Wanner, and W. Eugster (2008), Quantitative phenological observations of a mixed beech forest in northern Switzerland with digital photography, *J. Geophys. Res.*, *113*, G04004, doi:10.1029/2007JG000650.

1. Introduction

[2] Phenology is the study of recurring biological events in the biosphere and the causes of their timing [*Lieth*, 1976]. Historically, phenological studies have been performed in agriculture to document events such as plant emergence, fruiting and harvest. In recent decades phenology has become recognized as an important integrative method for assessing the impact of climate variability and climate change on ecosystems [*Menzel*, 2002; *Sparks and Menzel*, 2002]. Recent global warming has had significant effects on the seasonality of ecosystems [*Badeck et al.*, 2004; *Chuine et al.*, 2004; *Peñuelas and Filella*, 2001; *Zhang et al.*, 2007]. Time series analyses of selected variables such as green-up, maturity, senescence and dormancy, yield valuable information about ecosystem responses to climate and are widely used in climatological and ecological models [*Cleland et al.*, 2007; *Reed et al.*, 1994; *Schwartz*, 1994]. Plant phenology is strongly connected to the gas and water exchange of ecosystems [*Davis et al.*, 2003; *Knohl et al.*, 2003; *Moore et al.*, 1996]. Shifts in phenology can therefore significantly affect the global carbon and water cycle [*Baldocchi et al.*, 2005; *Churkina et al.*, 2005; *Piao et al.*, 2007]. Consequently, a knowledge and understanding of these phenological processes is needed for the parameterization of models used in climate predictions [*Arora and Boer*, 2005; *Lawrence and Slingo*, 2004a, 2004b; *Lu et al.*, 2001].

[3] Phenological ground observations span several decades, sometimes up to centuries [*Rutishauser et al.*, 2007], but they are often observer-biased [*Kharin*, 1976; *Menzel*, 2002]. Additionally, there is a significant decline in long-term observation sites due to a lack of volunteers for phenological field work. For two decades satellite remote sensing has been providing a globally integrated view of vegetation phenological states. However, this method still heavily depends on ground-based measurements for validation. Moreover, satellite images often have limited temporal and spatial coverage due to clouds, aerosols and other atmospheric- or sensor-related characteristics [e.g., *Ahl et al.*, 2006; *Fisher et al.*, 2006; *Studer et al.*, 2007; *Zhang et al.*, 2004, 2006]. Within the framework of the COST Action 725 (“Establishing a European Phenological Data Platform for Climatological Applications”), our project investigates the application of ground-based, commercially available digital cameras in observational procedures and quality assurance of phenological monitoring.

[4] Overall, the adoption of standard digital visible-light cameras in ecological research has been slow but recently

[1]Institute of Geography, University of Bern, Bern, Switzerland.
[2]Climate Analysis, Climate Services, Federal Office of Meteorology and Climatology MeteoSwiss, Zurich, Switzerland.
[3]Department of Atmospheric Science, Colorado State University, Fort Collins, Colorado, USA.
[4]Institute of Plant Sciences, ETH Zürich, Zurich, Switzerland.

0148-0227/08/2007JG000650

an increasing number of studies have used digital images from standard ground-based RGB (red, green and blue) cameras for vegetation studies. In an early approach *Brandhorst and Pinkhof* [1935] compared flowering and leaf development of common park trees with dated analog photography, and emphasized the use of photography for objective phenological monitoring. Vertical sky-ward wide-angle photography has been successfully used for monitoring changing light conditions in forests, Leaf Area Index (LAI) and canopy-closure-estimation [*Rich*, 1988, 1990; *Rich et al.*, 1993]. This technique was first used for forests by *Evans and Coombe* [1959] and is currently widely applied [*Jonckheere et al.*, 2004; *Nobis and Hunziker*, 2005; *Pellika*, 2001]. Vertical downward photography for the quantification of parameters such as vegetation fraction, LAI and biomass was performed by *Vanamburg et al.* [2006], *Zhou et al.* [1998], *Zhou and Robson* [2001], and *Behrens and Diepenbrock* [2006]. Other approaches analyzed vertical vegetation structures [*Zehm et al.*, 2003] and directional reflectance distributions of vegetation targets [*Dymond and Trotter*, 1997] with multiple digital images. The link between leaf pigmentation and digital images was found by *Kawashima and Nakatani* [1998] who estimated the chlorophyll content in leaves using a video camera. Net CO_2 uptake of moss was analyzed by *Graham et al.* [2006] with a RGB camera based upon the changes in reflected visible light (VIS) during moss drying and hydrating. The observation of phenological phases was first tested by *Adamsen et al.* [1999], who analyzed wheat senescence with a digital camera. *Sparks et al.* [2006] used monthly fixed-date, fixed-subject photographs to examine the correlation between plant phenology and mean monthly meteorological data. Digital camera images, phenology and satellite-based data were jointly analyzed by *Fisher et al.* [2006], who used multiple photographs, visually classified by independent observers, as validation data for satellite model estimates of phenological development. The latest research in webcam-based phenological monitoring was published by *Richardson et al.* [2007]. Digital webcam-images were successfully used for spring green-up tracking of a forest and jointly analyzed with FAPAR (fraction of incident photosynthetically active radiation absorbed by the canopy), broadband Normalized Difference Vegetation Index (NDVI) and the light-saturated rate of canopy photosynthesis, inferred from eddy covariance measurements at a flux tower site.

[5] Despite this pioneering work, the application of digital image analysis in vegetation phenology is still a young field. Previous studies mainly documented the conceptual use of area-integrated digital camera images in vegetation monitoring. Spatial and temporal uncertainty of digital images for continuous objective monitoring of phenological processes is still largely unknown. Species-specific image analysis, comparable with traditional phenological observations in a mixed forest canopy, has not yet been conducted. In this study we conducted species-specific phenological observation using digital photography, incorporating an uncertainty analysis, for a managed mixed forest in northern Switzerland. We focused on the forest spring phenology in 2005 and 2006, and aimed to identify leaf unfolding dates of the two dominant tree species, beech (*Fagus sylvatica* L.) and ash (*Fraxinus excelsior* L.). The automated observation of different species presented in our study here adds a further level of complexity and requires the separation of the phenological signal of single species from that of their surroundings. Given that within a mixed canopy the phenology of individual trees is locally adapted to environmental conditions such as light or tree age [e.g., *Kikuzawa*, 2003] we observed three ash and two beech trees using the camera. Additionally, we observed spring green-up of a mixed forested region located a few kilometers from the camera. Extending the work of previous studies, we conducted an uncertainty analysis, a species-dependant phenological observation including a year-to-year comparison, and interpreted the camera signal in detail. We were therefore able to examine both the potential and the limitations of this novel observation method.

2. Materials and Methods

2.1. Site Description

[6] The Lägeren research site is located at 47°28′49″N and 8°21′05″E at 682 m a.s.l. on the south slope of the Lägeren mountain, approximately 15 km northwest of Zürich, Switzerland. The south slope of the Lägeren mountain marks the boundary of the Swiss Plateau, which is bordered by the Jura and the Alps. Since 1986 the Lägeren site has been a permanent station of the Swiss air quality monitoring network (NABEL) [*Burkard et al.*, 2003]. A 45 m tall flux tower provides micrometeorological data at a high temporal resolution. Routine CO_2 and H_2O flux measurements as a contribution to the FLUXNET/CarboEuropeIP network started in April 2004 [*Eugster et al.*, 2007]. The mean annual temperature is 8°C. The mean annual precipitation is 1200 mm and the vegetation period is 170–190 days. The natural vegetation cover around the tower is a mixed beech forest. The western part is dominated by broad-leaved trees, mainly beech (*Fagus sylvatica* L.) and ash (*Fraxinus excelsior* L.). In the eastern part beech and Norway spruce (*Picea abies* (L.) Karst.) are dominant. The forest stand has a relatively high diversity of species, ages, and diameters [*Eugster et al.*, 2007].

[7] The vegetation cover within the camera's field of view predominantly consisted of beech, ash and silver fir (*Abies alba* Mill.). Understory vegetation varies, but during the study period it was dominated by bear garlic (*Allium ursinum* L.) and beech saplings.

2.2. Technical Setup

[8] On the uppermost platform of the Lägeren flux tower a standard digital 5-megapixel camera (NIKON Coolpix 5400, CCD sensor) was connected to a Linux-based computer and mounted in a weatherproof enclosure. The camera provides hourly digital raw images (2592 × 1944 pixels, 12 bit color resolution) of the Lägeren forest since autumn 2004. This camera was chosen because of its high sensor resolution, good quality optics and its ability to store images in uncompressed raw format. Quantitative image analysis requires the original and complete image information. Spatial or color compression (e.g., JPEG) by the camera's complex and proprietary image processing algorithms can potentially lead to information loss and nonlinearities [*Stevens et al.*, 2007]. Raw files contain the actual pixel data captured by the camera sensor, before it has undergone

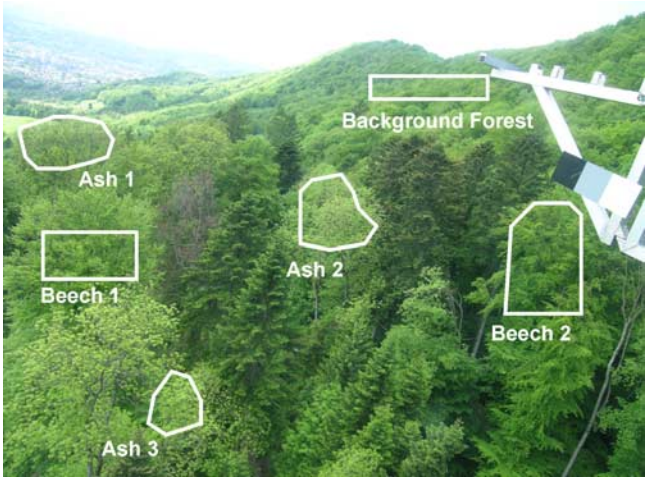

Figure 1. Sample camera image (24 May 2005) and regions of interests (ROIs) for image analysis. A color calibration panel facing south (right) is included in all images. ROIs are named after the dominant tree species.

any processing method. Furthermore, in the raw format, information such as white balance, saturation, color space or tonality are included as metadata and can be adjusted manually by the user following image capture. The field of view of the camera is approximately 60° wide and the view angle is tilted 25° below the horizon. A sample image is presented in Figure 1.

[9] Image capture was controlled by custom Perl (Practical Extraction and Report Language) scripts and the open-Source software gphoto2 (http://gphoto.org). To cope with diurnally and seasonally changing illumination conditions the camera was operated in the automatic exposure and aperture mode. The camera was pointed toward the west, looking at the southern slope of the Lägeren mountain. The sun therefore moved from behind to in front of the camera over the course of a day. As shown in Figure 1 a color calibration panel was included in the camera's field of view, but was not in the image analysis since reflection values were saturated on sunny days.

2.3. Image Analysis

[10] The NIKON raw image format (NEF) was processed into standard TIFF (Tagged Image File Format) without performing white balance, changes in color space, and without applying any automatic correction methods or filters, maintaining the original image information. The TIFF images (linearly scaled to 48 bit color resolution) provided a time series of digital data in the visible part of the electromagnetic spectrum (located approximately between 400 – 700 nm), at an hourly temporal resolution (excluding the dark hours). This scheduling was chosen so as to provide an adequate temporal resolution under limited data storage capacity.

[11] Data analysis was based on 64 midday images for 2005 and 67 images for 2006 between Day of Year (DOY) 101 (11 April) and 170 (19 June). Only the images taken near local noon time were used in order to minimize angular effects of the forest canopy's hemispherical directional reflectance function (HDRF) [*Chen et al.*, 2000]. This selection was supported by an uncertainty analysis examining the influence of diurnal illumination changes on camera-based phenology. Images with raindrops on the camera lens, images of very foggy days or days with snow cover were excluded from the time series analysis. Image analysis was conducted separately on each region in a set of regions of interest (ROIs) representing single tree species (Figure 1). Each ROI covered a specific set of species, and within each of these there was variation in vegetation during spring due to changing leaf coverage: closer trees masked those further away during green-up. As an extension to previous studies our analysis here explores the effects of these overlaying signals. Table 1 shows the different species included within the different ROIs. Regions of interest were named after the dominant tree species. We observed the phenology of three ash and two beech trees. The Beech 2 ROI and the Beech 3 ROI were mainly covered by the same tree, Beech 2 representing its upper crown and Beech 3 representing the lower crown and part of the understory vegetation. Beech trees generally show successive leafing, starting at the lower parts of the crown and moving up to the top of the crown [e.g., *Kikuzawa*, 1983; *Kikuzawa*, 1989; *Kikuzawa*, 2003]. Therefore we compared leafing dates of the Beech 2 ROI with those from the Beech 3 ROI. The Background Forest ROI was chosen in order to measure spatially integrated phenology characteristics of a heterogeneous area and to study the atmospheric disturbance effects at a larger distance from the camera.

[12] The image's color values (red, green and blue) were extracted and averaged across each ROI at daily intervals. Several vegetation indices have been developed to describe biomass amount and vegetation status. Since the camera's spectral sensitivity is limited to the visible part of the spectrum, we used the relative brightness of the green channel (GF: the ratio of the mean raw green value to the sum of the mean raw red, green and blue values):

$$GF = (G/(G + R + B))$$

[13] The exact spectral sensitivity of the NIKON Coolpix 5400 was not revealed by the manufacturer. The GF was computed from unsmoothed and noninterpolated mean color values for each ROI and was a suitable index for recording changes in vegetation state during spring. GF values were then plotted over time to describe changing phenology in the observed ROIs (Figure 2). Leaf emergence dates were (a) automatically determined using first and second derivatives ($\Delta GF/\Delta t$ and $\Delta^2 GF/\Delta t^2$) describing curvature changes (data not shown) and (b) by visual curvature shape interpretation. Generally leaf emergence is represented by the maximum value of the second derivative, that is, by the starting date of a significant GF increase (inflection point). The derivative methodology is very responsive to noise in the unsmoothed GF time series. It was successfully applied to Beech 1, 2 and 3, Background and Ash 3 ROIs. For the Ash 1 and 2 ROIs, leaf emergence dates were derived visually from the GF curvature shape as there was interference in the data from the earlier greening of background vegetation and understory (see in the following section).

Table 1. Regions of Interest Chosen for Image Analysis and the Main Vegetation Types Covered by the ROI[a]

Region of Interest	Number of Pixels	Main Vegetation Cover
Ash 1	58696	ash, mixed background vegetation of the lower forest
Ash 2	73924	ash, beech
Ash 3	50530	ash, silver fir
Beech 1	87048	beech, ash
Beech 2	137960	beech, silver fir, understory
Beech 3	21021	beech, understory
Background Forest	61313	beech, ash, maple

[a]ROI, regions of interest.

[14] Validation data were obtained from daily visual image interpretation combined with direct phenological observations of sample trees performed by the Forestry Office Wettingen. In 2006 the percentage of foliation in the upper, middle and lower part of Ash 3 and Beeches 1, 2 and 3 was documented between DOY 115 (25 April 2006) and 124 (4 May 2006) (data not shown). Leaf unfolding dates for the Ash 1 and 2 ROIs were visually estimated from imagery (Table 2). In 2005 validation data for all ROIs was visually estimated. Comparisons of field observations from 2006 with 2006 imagery served as reference. The human eye is readily able to differentiate between different stages of leaf emergence justifying visual image interpretation ("visual leaf unfolding" in Table 2). Visual interpretation of Background forest phenology further resulted in a higher uncertainty.

2.4. Uncertainty Analysis

[15] Pixel values and therefore GF values and leaf emergence dates are influenced by different biotic and abiotic factors. Uncertainties and variations on daily and hourly time-scales are thought to be mainly a result of abiotic factors such as changing ambient illumination conditions and wind influences.

[16] It can be assumed that the tree positions in the images changed due to tower and tree movements on windy days. Wind influences and natural leaf development led to different leaf inclination angles which may have influenced the levels of the extracted color values. We did not consider these influences within this study. To quantify uncertainties we focused on ambient illumination conditions. They affect results because of (a) changing radiation due to clouds and humidity, (b) diurnally and seasonally changing illumination angle, and (c) the limited dynamic range of the camera. Due to clouds and other atmospheric influences, such as water vapor content, the fraction of direct radiation changes over time. Its impact on photosynthetic activity and surface albedo was described e.g., by *Wang et al.* [2002], *Rocha et al.* [2004] and *Gamon et al.* [2006]. Also, dependencies of vegetation index values on illumination angles are well known [*Holben*, 1986]. Among others, *Holben and Kimes* [1986], *Jackson et al.* [1990] and *Schaaf and Strahler* [1994] have shown that surface anisotropic properties have a significant influence on surface reflectance measurements.

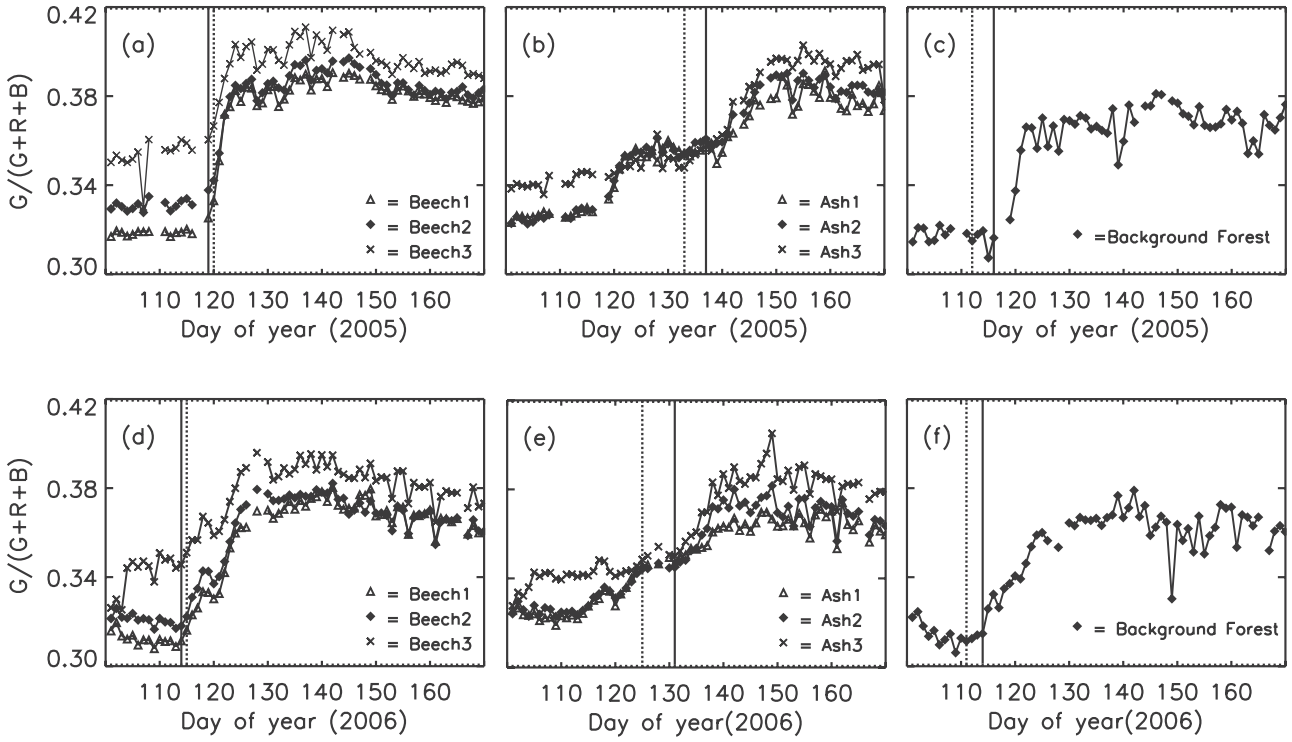

Figure 2. Green fraction (G/(G + R + B)) development during spring (DOY 100–170) for (a) beech-dominated ROIs in 2005 and (d) 2006, (b) ash-dominated ROIs in 2005 and (e) 2006 and (c) the Background Forest ROI in 2005 and (f) 2006. Solid vertical lines show mean GF-based leaf unfolding dates of the dominant tree species and dotted lines show mean unfolding dates provided by the validation data.

Table 2. Dates for Leaf Unfolding in 2005 and 2006 at the Lägeren Research Site[a]

	2005			2006		
ROI	Visual Leaf Unfolding (DOY)	GF-Based Leaf Unfolding (DOY)	Absolute Difference (days)	Visual Leaf Unfolding (DOY)	GF-Based Leaf Unfolding (DOY)	Absolute Difference (days)
Ash 1	138 (V)	140	2	128 (V)	131	3
Ash 2	131 (V)	139	8	124 (G)	131	7
Ash 3	129 (V)	133	4	124 (V)	131	7
Beech 1	121 (V)	119	−2	115 (G)	114	−1
Beech 2	120 (V)	119	−1	116 (G)	114	−2
Beech 3	119 (V)	119	0	115 (G)	113	−2
Background Forest	112 (V)	116	4	111 (V)	114	3
Mean error (days)			3			3.6

[a]Signals derived from digital imagery (GF-based leaf unfolding) and validation data (visual leaf unfolding) for the dominant vegetation type in each ROI are shown. Validation data are based on visual image interpretation (V) or based on ground observations (G).

The effect of the illumination angle is dependent on vegetation type, varies with spectral wavelength and is difficult to quantify [*Qi et al.*, 1995]. Using sample images we analyzed the variance due to both cloud conditions and to changing illumination angles, and quantified the impacts on the GF.

[17] We attempted to quantify the impact of changing fractions of diffuse radiation on the GF by comparing vegetation indices of (visually classified) ''cloudy'' and ''sunny'' images. We compared eight pairs of sunny and cloudy images from successive days taken at midday in the middle and at the end of the growing season. Except for the radiation, stable environmental conditions were assumed for the picture pairs. GF values of the images with higher diffuse radiation fractions (''cloudy'' days: DOY 144, 155, 163, 168, 209, 229, 234 in 2005) were subtracted from those with high direct radiation fraction (''sunny'' days: DOY 145, 154, 162, 167, 169, 208, 228, 235 in 2005). For each ROI and each pair of images the relative change of the GF was calculated (values normalized with the GF of the ''sunny'' images):

$$\Delta GF[\%] = \left(1 - GF_{cloudy}/GF_{sunny}\right) * 100[\%]$$

[18] Moreover, we hypothesized that changing diurnal illumination angles could have a significant impact on image pixel values and thus also on the GF. To test this assumption we calculated GF variation over five sunny days in the middle and at the end of the growing season of 2006 (DOY 163, 175, 181, 198 and 211). Mean RGB values were extracted from hourly digital images between 7:30 and 15:30 h.

3. Results

3.1. Temporal Spectral Response of the GF

[19] Figure 2 shows the GF curves and GF-derived leaf emergence dates for 2005 and 2006. The GF showed a characteristic curve shape, similar to spring leaf emergence phenology, and could therefore be used as a surrogate index for phenological phases. Generally the values showed species-specific seasonality. Short-term variations (noise component) were similar for each ROI.

[20] The Ash 1 ROI and the Ash 2 ROI displayed two consecutive pronounced rises in spring. The first rise was due to the leaf emergence of trees or understory vegetation in the background with earlier green-up dates, whereas the second increase was caused by the leaf flush of the ash. Figure 4 shows enlarged image data as an example of the Ash 2 ROI in spring 2006. This ROI was strongly influenced by a beech growing behind the ash, having an earlier leaf emergence which was partially visible in the space between the stem and bare branches of the ash tree in the foreground.

[21] Figure 3 shows the red and blue color values normalized to the overall brightness (red and blue fraction) for the ROIs Beech 1 and Ash 1 in 2005. The values were similar in 2006 (data not shown). For both species, the blue fraction (BF) decreased simultaneously with the increase of the GF during green-up while the red fraction (RF) remained approximately constant.

[22] After complete leaf expansion, when leaves were getting thicker, drier and darker and reached their delayed full photosynthetic activity [e.g., *Morecroft et al.*, 2003; *Schulze*, 1970], GF decreased in all ROIs, particularly in 2006. BF slightly increases and the RF decreases at that time.

[23] In 2006 the GF was generally lower than it had been in 2005. RF and BF values of the Background Forest ROI were highly scattered but curve characteristics were similar to the beech dominated ROIs (data not shown). Moreover, the Background Forest reflection values were higher than those of the regions next to the tower (data not shown). Since the camera adjusted exposure and aperture automatically, the background generally appeared brighter than the foreground, especially with high diffuse radiation fractions. At increasing distances from the camera higher atmospheric absorption and scattering of light occurs [*Janeiro et al.*, 2006]. Therefore the GF of the Background Forest ROI showed a less consistent curve compared to the other ROIs.

3.2. Validation of the GF

[24] Dates for the leaf emergence of the dominant tree species generally agreed well with validation data (Table 2). ROIs with similar dominant tree species showed similar GF curve shapes. GF curves in 2005 were more consistent than in 2006 (Figure 2). The estimation of transition dates in 2006 was more difficult due to irregularities in the GF curve. The mean error of observed onset compared with the validation data was 3 days in 2005 and 3.6 days in 2006. The maximum disagreement between validation and GF-

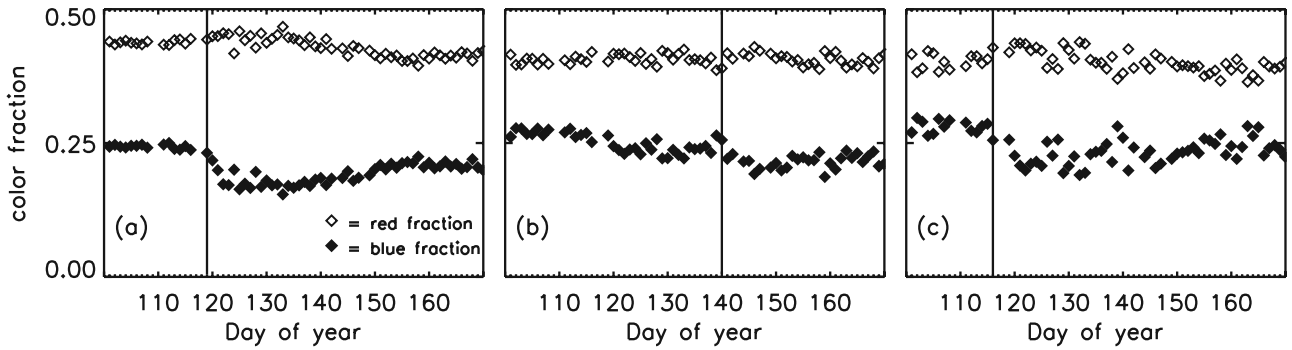

Figure 3. Red and blue color fractions exemplarily for (a) the Beech 1 ROI, (b) the Ash 1 ROI, and (c) the Background Forest ROI plotted over time (day of year) for 2005. Solid vertical line shows start of growing season date estimated from GF values.

based estimates was eight days in 2005 and seven days in 2006 for the Ash 2 ROI (Figure 4). GF-based dates for leaf unfolding for the beech-dominated ROIs showed better agreement with validation data than the ash-dominated ROIs. Because of missing images between DOY 116 and 119 in 2005 caused by a technical system failure, the derivation of the exact date for beech leaf unfolding was not possible. This does not affect the general finding that in both years the GF values in beech-dominated ROIs increased slightly earlier than indicated by the validation data. Possibly, this demonstrates the high objectivity and accuracy of the imagery for the observation of the budbreak. In field studies it was difficult to observe the exact date for first leaf appearance. However, the GF values may additionally be influenced by early leaf unfolding of beech saplings in the understory vegetation. In contrast, GF values for ash-dominated ROIs increased after leaf unfolding was observed in the field. As noted above, GF already increased for the ash-dominated ROIs when other vegetation components such as the understory or beech trees were greening up. Therefore, after leaf emergence of the ash tree, the GF values only increased when ash leaves started covering branches, stem and other previously nongreen parts in the ROI. This is also the most likely cause for the greater disagreement between the ash-dominated regions with the validation data.

[25] The mean date of leaf unfolding was five days earlier in 2006 than in 2005 for beech-dominated ROIs and six days earlier for ash-dominated ROIs. For the Background Forest ROI leaf emergence started two days earlier in 2006. Maximum GF values of the observed ROIs were reached between the middle and the end of May in both years. Within species, the GF-based dates for the start of the growing season dates were very similar. The delayed green-up of the Ash 1 ROI and the earlier green-up of the Ash 3 ROI in 2005 agreed well with validation data. In 2006 leaf emergence in the lower crown layers, represented by the Beech 2 ROI, happened earlier than in the upper crown layers, represented by the Beech 3 ROI. In 2005 this difference between the Beech 2 and the Beech 3 ROIs did not show up in the GF values, probably because of the missing images between DOY 116 and 119.

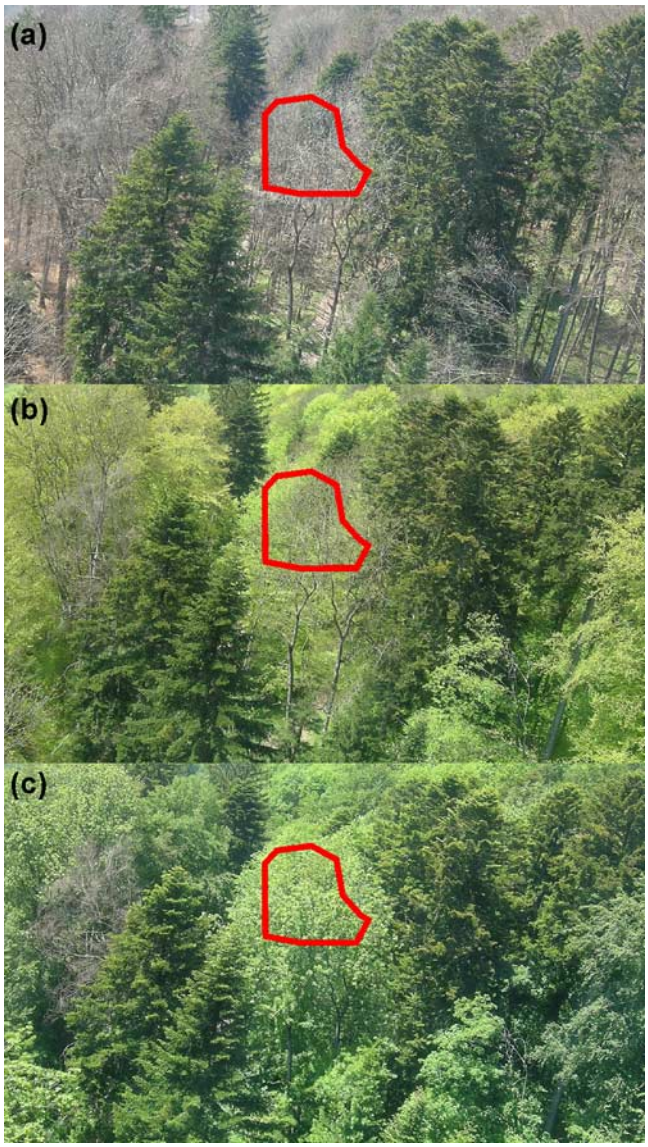

Figure 4. Enlarged images of the Ash 2 ROI. Successive masking of the beech growing behind the ash: (a) no leaves (14 April 2006), (b) beech leaves unfolded (4 May 2006), and (c) ash masks beech (8 June 2006).

Table 3. Mean and Maximum Relative Change of the Green Fraction Due to Clouds in 2005[a]

ROI	Mean ΔGF (%)	Maximum ΔGF (%)
Ash 1	1.2	2.7
Ash 2	0.5	1.3
Ash 3	0.6	1.8
Beech 1	0.6	1.1
Beech 2	0.5	1.2
Beech 3	0.8	1.8
Background Forest	1.5	3.7

[a]Results for each ROI (region of interest) are obtained by pairwise comparison of 16 images with different illumination conditions. GF, green fraction.

3.3. Uncertainty Analysis

[26] To quantify the impact of the diffuse radiation fraction on the GF values we compared eight pairs of sunny and cloudy images. Resulting mean and maximum estimated GF changes for each ROI are given in Table 3. As the chosen images do not represent extremely contrasting sky conditions, the values represent average uncertainty rather than maximum uncertainty. The impact was highest for the furthest ROIs, such as the Background Forest and Ash 1. Their greater distances from the camera made these parts of the images more susceptible to the effects of water vapor absorption and scattering processes (particularly on cloudy days with higher air humidity). Therefore, these parts generally appeared brighter, resulting in a higher impact on the GF. Also, the spatial variability caused by stronger contrasts between shadowed and sunny areas seemed to be compensated by the averaging of color values over the observed ROIs.

[27] To test the impact of changing illumination angles we calculated the diurnal course of GF values over five sunny days of 2006 between 7:30 and 15:30 h (Figure 5). Generally, GF values first increased and then decreased again. Maximum GF values were reached before midday, except for the Beech 3 ROI (Figure 5b). To quantify the impact the coefficient of variation (in percent) was calculated for each ROI. Largest variations were found in the Beech 3 ROI (Table 4). This ROI was significantly affected by shadow effects. All ROIs showed significant dependencies on the illumination angle. This supports our choice of using only noontime images. The computed values displayed, not only effects of daily changes in illumination angles, but also revealed an effect of the seasonal shift in the sun's position. For ash-dominated ROIs and the Background Forest ROI GF values generally decreased from June to July. Beech-dominated ROIs showed first a decrease between DOY 163 and 175, and afterwards remained constant. Furthermore, varying radiation values, leaf inclination angles and environmental conditions were influencing the result. GF

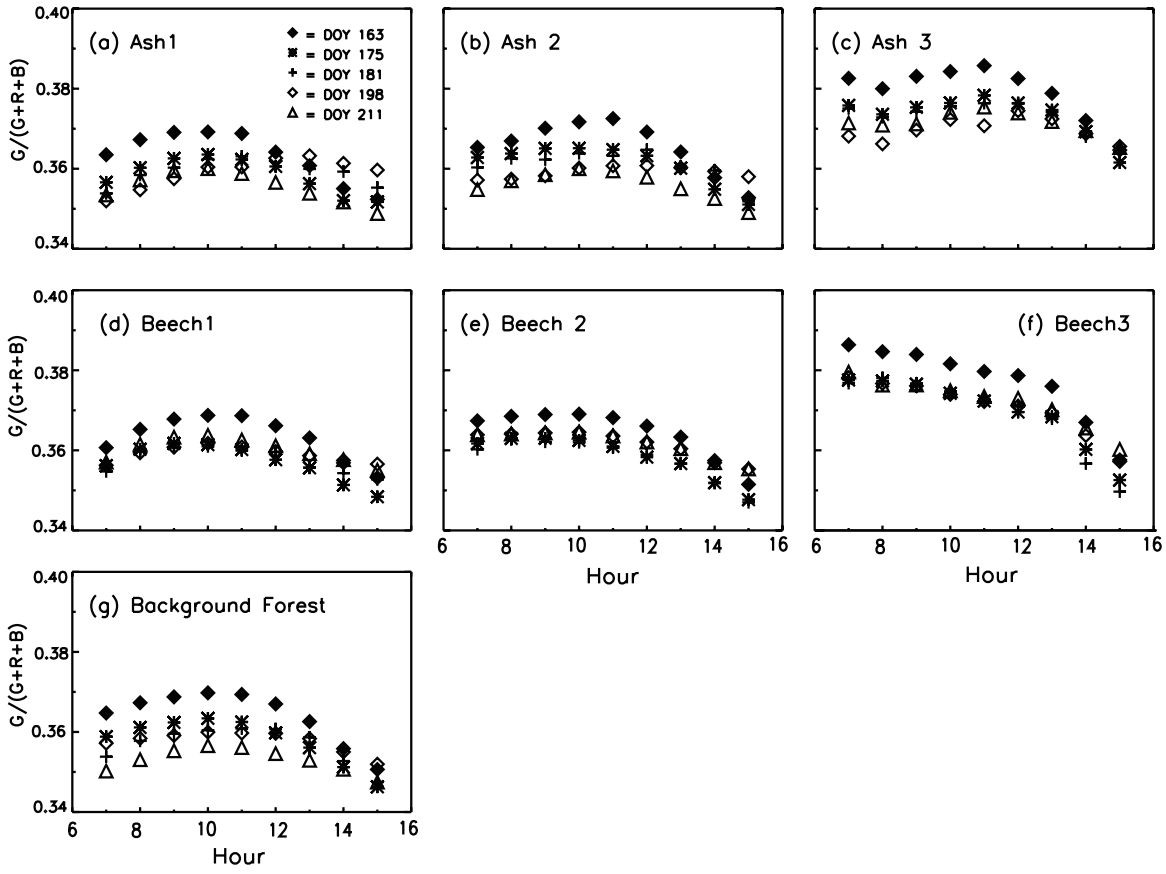

Figure 5. Variation of the green fraction (G/(G + R + B)) during DOY 163 (12 June), 175 (24 June), 181 (30 June), 198 (17 July) and 211 (30 July) for each ROI.

Table 4. GF Coefficient of Variation in 2006 Due to Changing Illumination Angle Over the Day[a]

Region of Interest	DOY 163	DOY 175	DOY 181	DOY 198	DOY 211
Ash 1	1.9	1.4	1.1	1.2	1.2
Ash 2	2.0	1.5	1.2	0.4	1.1
Ash 3	2.0	1.5	1.2	0.9	0.9
Beech 1	1.7	1.4	1.0	0.6	0.9
Beech 2	1.9	1.7	1.7	1.1	1.1
Beech 3	2.8	2.5	3.0	2.0	1.8
Background Forest	2.0	1.8	1.4	0.8	1.0

[a]GF variation was calculated over 5 sunny days in the middle and at the end of the growing season.

values were generally more sensitive to illumination angles than to variations in the diffuse radiation fraction.

4. Discussion

[28] The image-based estimates of leaf emergence dates suggest that camera-based observation of a forest-canopy provides temporally accurate and objective phenological information at the species level. In this study, we focused on the estimation of the leaf flushing date of two deciduous tree species. Image data provides a variety of information about vegetation development. However, without knowing the spectral sensitivity of the camera's sensor, image color values do not allow us to draw firm conclusions with respect to biogeochemical processes such as photosynthetic efficiency [*Kira and Kumura*, 1985]. Nevertheless, the GF was found to be a reliable measure for the timing of biophysical processes such as leaf emergence and expansion in spring. Maximum GF values represent vegetation cover fraction and maximum canopy closure within the ROI. Therefore the GF allows, within a specific uncertainty due to mixed species, objective statements about phenology and leaf emergence rates. These estimates can be compared with data obtained by ground-based field studies. Moreover the GF describes optical leaf color such as leaf darkening due to chlorophyll accumulation [e.g., *Bray and Sanger*, 1961; *Bray et al.*, 1966] and changes in the leaf surface due to maturity and aging processes [e.g., *Ito et al.*, 2006]. However, the decrease in the GF after complete leaf expansion which was observable in all ROIs may have been additionally influenced by seasonal changes of midday sun angles as described in our uncertainty analysis.

[29] Owing to the mixed background signal from the variety of species, GF values did not provide a method for estimating the leaf area index [*Chen and Black*, 1992] for the ROIs. We found a generally lower green fraction in 2006. Field studies showed that 2006 was a mast year for the beech and possibly the ash. Fruiting beech trees generally have more transparent crowns because a proportion of the buds have developed into flowers and the leaf size is reduced [*Innes*, 1994]. This could be a possible explanation for the lower GF levels in these ROIs. However, observed similarity of short-term GF variations demonstrate the larger influence of environmental conditions, e.g., illumination conditions. Therefore, it is also reasonable that the lower GF values were caused by abiotic factors.

[30] Not only species-specific but also individual leaf unfolding dates could be observed. Individual trees experience different green-up dates due to genetic differences and based on their position within the forest canopy. The GF-based leaf unfolding date was up to one week later for the Ash 1 ROI in 2005 compared to the other ash-dominated ROIs. This ROI was mainly covered by a relatively free-standing ash tree compared with the other ash trees within the camera's field of view. Although the delayed leaf unfolding could not be shown with GF values for 2006, the observation is consistent with the validation data. Our results agree with studies from *Brügger et al.* [2003] about the phenological variability within one species due to the genetic differences and the different social positions of the individual trees. Successive leafing processes moving from lower to upper parts of the foliage could be observed for beeches during field work but only showed up in the image data for 2006. The mean error for the estimation of the leaf unfolding dates was larger than the variation in the leaf unfolding dates for the different parts of the crown.

[31] Our study also found less consistent GF curves for the Background Forest ROI located a few kilometers from the camera compared to the other ROIs which were next to the tower. The higher noise component of the GF for this ROI made an automated detection of phenological transition dates much more difficult. However, since the Background Forest ROI covers a set of different tree species, GF values probably represent the maximum time span of leaf development for the sampled trees.

[32] The GF is strongly influenced by the different species included within the ROIs. Therefore the installation of phenological cameras should be performed cautiously with respect to the different species included in the cameras field of view. An observation with camera images of the understory green-up provides useful additional information. For instance, since the phenological studies with satellite images based on the NDVI [e.g., *Tucker*, 1979] are strongly influenced by the earlier green-up of understory and saplings, analyses of the image's color values can be used for objective satellite data validation. However, comparisons with satellite data should be performed with respect to the timing of phenological processes rather than as a quantitative comparison. For a realistic validation and for the comparison of imagery from different cameras the spectral calibration of the camera model under use would be required [*Stevens et al.*, 2007].

[33] In recent years eddy covariance measurements have been performed worldwide at flux tower sites for calculating local and regional carbon dioxide and water balances. In this context, shifts in phenology could significantly affect annual carbon uptake and water cycling [i.e., *Baldocchi et al.*, 2005; *Churkina et al.*, 2005; *Gu et al.*, 2003; *Keeling et al.*, 1996; *Morecroft et al.*, 2003; *Niemand et al.*, 2005; *Piao et al.*, 2007; *White et al.*, 1999]. Therefore *Baldocchi et al.* [2005] suggested installing video cameras at flux tower sites for continuous monitoring of the canopy state. Since photographic cameras have a much better image resolution and quality than video cameras, our study suggests that still digital cameras may be better suited for this purpose. However, since measurements of the net ecosystem carbon dioxide exchange are strongly related to leaf gas exchange and therefore to photosynthetic activity and biomass, comparisons with GF values from standard digital images should also be based on the timing of phenological phases

rather than on quantitative data. We believe that the installation of digital cameras can be used to bridge the gap between CO_2 flux measurements at ecosystem scale and satellite-based vegetation monitoring at a regional scale. Continuous time series of digital images of the forest canopy could complement terrestrial monitoring of gas and water exchanges at forest sites.

[34] We found a considerable sensitivity of the GF to illumination conditions, mainly to changing sun angles. The interpretation of the result of the uncertainty analysis is difficult due to complex canopy structures [*Leuchner et al.*, 2007] and the different geometric positions of the trees relative to the sun and the camera within the canopy at midday. Further research with respect to the quantification of these influences is needed. Changing fractions of different tree species over time also have to be considered. Illumination conditions need to be quantified as a base for comparisons. Visual estimates of tree phenology for ground truthing may be hampered by the same light and visibility problems as digital camera image analysis. Weather conditions are rarely uniform and especially fog, sun angle and general brightness have a significant influence on the color sensitivity of the human eye. Considering all these aspects together, it becomes clear that, despite there is moderate uncertainty in the GF values, GF curves can be used for detection of leaf emergence dates which are typically accurate to within a few days from the validation data.

5. Conclusions

[35] We found that the use of consumer-grade digital cameras offers the possibility of monitoring phenology with high temporal and spatial accuracy with respect to the phenological state of leaf emergence of individual deciduous trees. Our study clearly showed that changing illumination conditions introduce a moderate uncertainty in phenological estimates. By choosing pictures taken at a particular hour every day to monitor vegetation development, this uncertainty can be minimized. Furthermore our results suggest that species-dependant phenological observations in mixed forests are successful if overlaying signals of the different species covered by a specific analyzed ROI are detected and separated. The camera should be mounted within an appropriate distance from the observed canopy to minimize scattering of the color values which aggravates automated detection of phenological transition dates.

[36] Based on this case study for a European mixed forest we anticipate that a network of digital cameras could provide inexpensive, spatially representative and objective information with the required temporal resolution for phenological applications at species-level and process-based ecosystem research. In future studies the application of digital camera images at sites with different dominant vegetation types such as grassland sites or in agriculture should be analyzed. From a technical viewpoint, noise removal, algorithm development (e.g., by optimized filtering methods) to automate the detection of phenological phases, and the standardization of these algorithms for public use, should receive special attention. Since these aspects are related to data processing and not to data acquisition, we are convinced that phenological monitoring with digital cameras is a suitable method to be used in a network of automated phenological observation sites.

[37] **Acknowledgments.** This project is funded by the Federal Department of Home Affairs FDAA: State Secreteriat for Education and Research SER, SBF CO5.0032. We are grateful to the National Center of Competence in Research on Climate (NCCR Climate) for supporting this project. This publication was supported by the Foundation Marchese Francesco Medici del Vascello. We acknowledge Paul Messerli for publication sponsorship. We are grateful to Philipp Vock (Forestry Office, Wettingen) for field work and validation data.

References

Adamsen, F. J., P. J. Pinter, E. M. Barnes, R. L. LaMorte, G. W. Wall, S. W. Leavitt, and B. A. Kimball (1999), Measuring wheat senescence using a digital camera, *Crop Sci.*, *39*, 719–724.

Ahl, D. E., S. T. Gower, S. N. Burrows, N. V. Shabanov, R. B. Myneni, and Y. Knyazikhin (2006), Monitoring spring canopy phenology of a deciduous broadleaf forest using MODIS, *Remote Sens. Environ.*, *104*, 88–95.

Arora, V. K., and G. J. Boer (2005), A parameterization of leaf phenology for the terrestrial ecosystem component of climate models, *Global Change Biol.*, *11*, 39–59.

Badeck, F. W., A. Bondeau, K. Böttcher, D. Doktor, W. Lucht, J. Schaber, and S. Sitch (2004), Responses of spring phenology to climate change, *New Phytol.*, *162*, 295–309.

Baldocchi, D. D., et al. (2005), Predicting the onset of net carbon uptake by deciduous forests with soil temperature and climate data: A synthesis of FLUXNET data, *Int. J. Biometeorol.*, *49*(6), 377–387.

Behrens, T., and W. Diepenbrock (2006), Using digital image analysis to describe canopies of winter oilseed rape (Brassica napus L.) during vegetative developmental stages, *J. Agron. Crop Sci.*, *192*, 295–302.

Brandhorst, A. L., and M. Pinkhof (1935), Exact determination of phytophenological stages, *Acte Phaenol.*, *3*, 101–109.

Bray, J. R., and J. E. Sanger (1961), Light reflectivity as an index of chlorophyll content and production potential of various kinds of vegetation, *Proc. Minn. Acad. Sci.*, *29*, 222–226.

Bray, J. R., J. E. Sanger, and A. L. Archer (1966), The visible albedo of surfaces in central Minnesota, *Ecology*, *47*(4), 524–531.

Brügger, R., M. Dobbertin, and N. Krauchi (2003), Phenological variation of forest trees, in *Phenology: An Integrative Environmental Science*, edited by M. D. Schwartz, pp. 255–268, Kluwer Acad., Dordrecht, Netherlands.

Burkard, R., P. Bützberger, and W. Eugster (2003), Vertical fogwater flux measurements above an elevated forest canopy at the Lägeren research site, Switzerland, *Atmos. Environ.*, *37*, 2979–2990.

Chen, J. M., and T. A. Black (1992), Defining leaf area index for non-flat leaves, *Plant Cell Environ.*, *15*(4), 421–429.

Chen, J. M., X. Li, T. Nilsonn, and A. Strahler (2000), Recent advances in geometrical optical modelling and its applications, *Remote Sens. Rev.*, *18*, 227–262.

Chuine, I., P. Yiou, N. Viovy, and B. Seguin (2004), Grape ripening as a past climate indicator, *Nature*, *432*, 289–290.

Churkina, G., D. Schimel, B. H. Braswell, and X. Xiao (2005), Spatial analysis of growing season length control over net ecosystem exchange, *Global Change Biol.*, *11*, 1777–1787.

Cleland, E. E., I. Chuine, A. Menzel, H. A. Mooney, and D. Mark (2007), Shifting plant phenology in response to global change, *Trends Ecol. Evol.*, *22*(7), 357–365.

Davis, K. J., P. S. Bakwin, C. Yi, B. W. Berger, C. Zhao, R. M. Teclaw, and J. G. Isebrands (2003), The annual cycles of CO_2 and H_2O exchange over a northern mixed forest as observed from a very tall tower, *Global Change Biol.*, *9*, 1278–1293.

Dymond, J. R., and C. M. Trotter (1997), Directional reflectance of vegetation measured by a calibrated digital camera, *Appl. Opt.*, *36*(18), 4314–4319.

Eugster, W., K. Zeyer, M. Zeeman, P. Michna, A. Zingg, N. Buchmann, and L. Emmenegger (2007), Nitrous oxide net exchange in a beech dominated mixed forest in Switzerland measured with a quantum cascade laser spectrometer, *Biogeosciences Discuss.*, *4*, 1167–1200.

Evans, G. C., and D. E. Coombe (1959), Hemispherical and woodland canopy photography and the light climate, *J. Ecol.*, *47*, 103–113.

Fisher, J. I., J. F. Mustard, and M. A. Vadeboncoeur (2006), Green leaf phenology at Landsat resolution: Scaling from the field to the satellite, *Remote Sens. Environ.*, *100*, 265–279.

Gamon, J. A., Y. Cheng, H. Claudio, L. MacKinney, and D. A. Sims (2006), A mobile tram system for systematic sampling of ecosystem optical properties, *Remote Sens. Environ.*, *103*, 246–254.

Graham, E., M. P. Hamilton, B. D. Mishler, P. W. Rundel, and M. H. Hansen (2006), Use of a networked digital camera to estimate net CO_2 uptake of a desiccation-tolerant moss, *Int. J. Plant Sci.*, *167*(4), 751–758.

Gu, L., W. M. Post, D. Baldocchi, T. A. Black, S. B. Verma, T. Vesala, and S. C. Wofsy (2003), Phenology of vegetation photosynthesis, in *Phenology: An Integrative Environmental Science*, edited by M. D. Schwartz, pp. 467–485, Kluwer Acad., Dordrecht, Netherlands.

Holben, B. N. (1986), Characteristics of maximum-value composite images from temporal AVHRR data, *Int. J. Remote Sens.*, *7*(11), 1417–1434.

Holben, B., and D. Kimes (1986), Directional reflectance response in AVHRR red and near-IR bands for three cover types and varying atmospheric conditions, *Remote Sens. Environ.*, *19*, 213–236.

Innes, J. L. (1994), The occurrence of flowering and fruiting on individual trees over 3 years and their effects on subsequent crown conditions, *Trees (Berl.)*, *8*, 139–150.

Ito, A., H. Muraoka, H. Koizumi, N. Saigusa, S. Murayama, and S. Yamamoto (2006), Seasonal variation in leaf properties and ecosystem carbon budget in a cool-temperate deciduous broad-leaved forest: Simulation analysis at Takayama site, Japan, *Ecol. Res.*, *21*, 137–149.

Jackson, R. D., P. M. Teillet, P. N. Slater, G. Fedosejevs, M. F. Jasinski, J. K. Aase, and M. S. Moran (1990), Bidirectional measurements of surface reflectance for view angle corrections of oblique imagery, *Remote Sens. Environ.*, *32*, 189–202.

Janeiro, F. M., F. Wagner, and A. M. Silva (2006), Visibility measurements using a commercial digital camera, paper presented at Conference on Visibility, Aerosols, and Atmospheric Optics, Assoc. for Aerosol Res., UNIQA Group Austria, Vienna, Austria, 4–6 Sept.

Jonckheere, I., S. Fleck, K. Nackaerts, B. Muys, P. Coppin, M. Weiss, and F. Baret (2004), Review of methods for in situ leaf area index determination, Part I. Theories, sensors and hemispherical photography, *Agric. For. Meteorol.*, *121*, 19–35.

Kawashima, S., and M. Nakatani (1998), An algorithm for estimating chlorophyll content in leaves using a video camera, *Ann. Bot. (Lond.)*, *81*, 49–54.

Keeling, C. D., J. F. S. Chin, and T. P. Whorf (1996), Increased activity of northern vegetation inferred from atmospheric CO_2 measurements, *Nature*, *382*, 146–149.

Kharin, N. G. (1976), Mathematical models in phenology, *J. Biogeogr.*, *3*, 357–364.

Kikuzawa, K. (1983), Leaf survival of woody plants in deciduous broad-leaved forests. 1. Tall trees, *Can. J. Bot.*, *61*, 2133–2139.

Kikuzawa, K. (1989), Ecology and evolution of phenological pattern, leaf longevity and leaf habit, *Evol. Trends Plants*, *3*, 105–110.

Kikuzawa, K. (2003), Phenological and morphological adaptations to the light environment in two woody and two herbaceous plant species, *Funct. Ecol.*, *17*(1), 29–38.

Kira, T., and A. Kumura (1985), Dry matter production and efficiency in various types of plant canopies, in *Plant Research and Agroforestry*, edited by P. A. Huxley, pp. 347–364, Int. Counc. for Res. in Agrofor., Nairobi, Kenya.

Knohl, A., E. Schulze, O. Kolle, and N. Buchmann (2003), Large carbon uptake by an unmanaged 250-year-old deciduous forest in Central Germany, *Agric. For. Meteorol.*, *118*, 151–167.

Lawrence, D. M., and J. M. Slingo (2004a), An annual cycle of vegetation in a GCM. Part I: Implementation and impact on evaporation, *Clim. Dyn.*, *22*(2–3), 87–105.

Lawrence, D. M., and J. M. Slingo (2004b), An annual cycle of vegetation in a GCM. Part II: Global impacts on climate and hydrology, *Clim. Dyn.*, *22*(2–3), 107–122.

Leuchner, M., A. Menzel, and H. Werner (2007), Quantifying the relationship between light quality and light availability at different phenological stages within a mature mixed forest, *Agric. For. Meteorol.*, *142*, 35–44.

Lieth, H. H. (1976), Contributions to phenology seasonality research, *Int. J. Biometeorol.*, *20*(3), 197–199.

Lu, L., R. A. Pielke Sr., G. Liston, W. Parton, D. Ojima, and M. Hartman (2001), Implementation of a two-way interactive atmospheric and ecological model and its application to the central United States, *J. Clim.*, *14*, 900–919.

Menzel, A. (2002), Phenology: Its importance to the global change community, *Clim. Change*, *54*, 379–385.

Moore, K. E., D. R. Fitzjarrald, R. K. Sakai, M. L. Goulden, J. W. Munger, and S. C. Wofsy (1996), Seasonal variation in radiative and turbulent exchange at a deciduous forest in central Massachusetts, *J. Appl. Meteorol.*, *35*, 122–134.

Morecroft, M. D., V. J. Stokes, and J. I. L. Morison (2003), Seasonal changes in the photosynthetic capacity of canopy oak (Quercus robur) leaves: The impact of slow development on annual carbon uptake, *Int. J. Biometeorol.*, *47*, 221–226.

Niemand, C., B. Köstner, H. Prasse, T. Grünwald, and C. Bernhofer (2005), Relating tree phenology with annual carbon fluxes at Tharandt forest, *Meteorol. Z.*, *14*(2), 197–202.

Nobis, M., and U. Hunziker (2005), Automatic thresholding for hemispherical canopy-photographs based on edge detection, *Agric. For. Meteorol.*, *128*, 243–250.

Pellika, P. (2001), Application of vertical skyward wide-angle photography and airborne video data for phenological studies of beech forests in the German Alps, *Int. J. Remote Sens.*, *22*(14), 2675–2700.

Peñuelas, J., and I. Filella (2001), Responses to a warming world, *Science*, *294*, 793–795.

Piao, S., P. Friedlingstein, P. Ciais, N. Viovy, and J. Demarty (2007), Growing season extension and its impact on terrestrial carbon cycle in the Northern Hemisphere over the past 2 decades, *Global Biogeochem. Cycles*, *21*, GB3018, doi:10.1029/2006GB002888.

Qi, J., M. S. Moran, F. Cabot, and G. Dedieu (1995), Normalization of sun/view angle effects using spectral albedo-based vegetation indices, *Remote Sens. Environ.*, *52*, 207–217.

Reed, B. C., J. F. Brown, D. VanderZee, T. R. Loveland, J. W. Merchant, and D. O. Ohlen (1994), Measuring phenological variability from satellite imagery, *J. Veg. Sci.*, *5*(5), 703–714.

Rich, P. M. (1988), Video image analysis of hemispherical canopy photography, in *First Special Workshop on Videography*, edited by P. W. Mausel, pp. 84–95, American Soc. for Photogramm. and Remote Sens., Terre Haute, Ind.

Rich, P. M. (1990), Characterizing plant canopies with hemispherical photography, in *Instrumentation for Studying Vegetation Canopies for Remote Sensing in Optical and Thermal Infrared Regions*, edited by N. S. Goel and J. M. Norman, *Remote Sens. Rev.*, *5*(1), 13–29.

Rich, P. M., D. B. Clark, D. A. Clark, and S. Oberbauer (1993), Long-term study of solar radiation regimes in a tropical wet forest using quantum sensors and hemispherical photography, *Agric. For. Meteorol.*, *65*, 107–127.

Richardson, A. D., J. P. Jenkins, B. H. Braswell, D. Y. Hollinger, S. V. Ollinger, and M. Smith (2007), Use of digital webcam images to track spring green-up in a deciduous broadleaf forest, *Oecologia*, *152*, 323–334.

Rocha, A. V., H. B. Su, C. S. Vogel, H. P. Schmid, and P. S. Curtis (2004), Photosynthetic and water use efficiency responses to diffuse radiation by an aspen-dominated northern hardwood forest, *For. Sci.*, *50*(6), 793–801.

Rutishauser, T., J. Luterbacher, F. Jeanneret, C. Pfister, and H. Wanner (2007), A phenology-based reconstruction of inter-annual changes in past spring seasons, *J. Geophys. Res.*, *112*, G04016, doi:10.1029/2006JG000382.

Schaaf, C. B., and A. H. Strahler (1994), Validation of bidirectional and hemispherical reflectances from a geometric-optical model using ASAS imagery and pyranometer measurements of a spruce forest, *Remote Sens. Environ.*, *49*, 138–144.

Schulze, E. (1970), Der CO_2-Gaswechsel der Buche, *Flora*, *159*, 177–232.

Schwartz, M. (1994), Monitoring global change with phenology: The case of the spring green wave, *Int. J. Biometeorol.*, *38*(1), 18–22.

Sparks, T. H., and A. Menzel (2002), Observed changes in seasons: An overview, *Int. J. Climatol.*, *22*, 1715–1725.

Sparks, T. H., K. Huber, and P. J. Croxton (2006), Plant development scores from fixed-date photographs: The influence of weather variables and recorder experience, *Int. J. Biometeorol.*, *50*, 275–279.

Stevens, M., C. A. Párraga, I. C. Cuthill, J. C. Partridge, and T. S. Troscianko (2007), Using digital photography to study animal coloration, *Biol. J. Linn. Soc. Lond.*, *90*, 211–237.

Studer, S., R. Stöckli, C. Appenzeller, and P. L. Vidale (2007), A comparative study of satellite and ground-based phenology, *Int. J. Biometeorol.*, *51*(5), 405–414.

Tucker, C. J. (1979), Red and photographic infrared linear combinations for monitoring vegetation, *Remote Sens. Environ.*, *8*, 127–150.

Vanamburg, L. K., M. J. Trlica, R. M. Hoffer, and M. A. Weltz (2006), Ground based digital imagery for grassland biomass estimation, *Int. J. Remote Sens.*, *27*(5), 939–950.

Wang, S., S. G. Leblanc, R. Fernandes, and J. Cihlar (2002), Diurnal variation of direct and diffuse radiation and its impact on surface albedo, *IEEE Int. Geosci. Remote Sens. Symp.*, *6*, 3224–3226.

White, M. A., S. W. Running, and P. E. Thornton (1999), The impact of growing-season length variability on carbon assimilation and evapotranspiration over 88 years in the eastern U.S. deciduous forest, *Int. J. Biometeorol.*, *42*, 139–145.

Zehm, A., M. Nobis, and A. Schwabe (2003), Multiparameter analysis of vertical vegetation structure based on digital image processing, *Flora*, *198*, 142–160.

Zhang, X., M. A. Friedl, C. B. Schaaf, and A. H. Strahler (2004), Climate controls on vegetation phenological patterns in northern mid- and high latitudes inferred from MODIS data, *Global Change Biol.*, *10*, 1133–1145.

Zhang, X., M. A. Friedl, and C. B. Schaaf (2006), Global vegetation phenology from Moderate Resolution Imaging Spectroradiometer (MODIS): Evaluation of global patterns and comparison with in situ measurements, *J. Geophys. Res.*, *111*, G04017, doi:10.1029/2006JG000217.

Zhang, X., D. Tarpley, and J. T. Sullivan (2007), Diverse responses of vegetation phenology to a warming climate, *Geophys. Res. Lett.*, *34*, L19405, doi:10.1029/2007GL031447.

Zhou, Q., and M. Robson (2001), Automated rangeland vegetation cover and density estimation using ground digital images and a spectral-contextual classifier, *Int. J. Remote Sens.*, *22*(17), 3457–3470.

Zhou, Q., M. Robson, and P. Pilesji (1998), On the ground estimation of vegetation cover in Australian rangelands, *Int. J. Remote Sens.*, *19*(9), 1815–1820.

H. E. Ahrends, R. Brügger, F. Jeanneret, P. Michna, J. Schenk, and H. Wanner, Institute of Geography, University of Bern, Hallerstrasse 12, CH-3012 Bern, Switzerland. (ahrends@giub.unibe.ch)

W. Eugster, Institute of Plant Sciences, ETH Zürich, Universitätsstrasse 2, CH-8092 Zürich, Switzerland.

R. Stöckli, Climate Analysis, Climate Services, Federal Office of Meteorology and Climatology MeteoSwiss, Krähbühlstrasse 58, CH-8044 Zürich, Switzerland.